Available online at www.sciencedirect.com
ScienceDirect
Bioelectrochemistry 69 (2006) 148 – 157
Bioelectrochemistry
www.elsevier.com/locate/bioelechem

Electroreduction of dioxygen on Au_{nano}–DNA film electrode in acidic electrolyte

Fang Wang [a,b], Jia Zhao [a], Yanxia Xu [a], Shengshui Hu [a,b,*]

[a] Department of Chemistry, Wuhan University, Wuhan 430072, PR China
[b] State Key Laboratory of Transducer Technology, Chinese Academy of Sciences, Beijing 100080, PR China

Received 7 September 2005; received in revised form 11 January 2006; accepted 16 January 2006
Available online 23 February 2006

Abstract

The colloidal Au nanoparticles–deoxyribonucleic acid (Au_{nano}–DNA) film modified glassy carbon electrode (GCE) has been fabricated and the electrochemical reduction of dioxygen (O_2) at this modified GCE has been studied in 0.2 mol/L air-saturated acetate buffer (pH=5.2) using cyclic voltammetry (CV), chronocoulometry (CC), linear scan voltammetry (LSV) and rotating disk electrode (RDE) as diagnostic techniques. The modified electrode shows excellent enhancement effect towards the reduction of dioxygen to hydrogen peroxide (H_2O_2), and the overpotential is lower than that at bare GCE. A well-defined dioxygen reduction peak appeared at about −0.24 V. Based on experimental results, a reaction mechanism is proposed and discussed.

Keywords: Electrochemical reduction; Dioxygen; Au nanoparticles; Glassy carbon electrode (GCE)

1. Introduction

Dioxygen reduction is very important to many electrochemical processes, such as fuel cells and metal-air batteries [1–5]. It may be analyzed in terms of two main reaction pathways involving direct four-electron and two two-electron steps reduction pathways. In fact, a series of intermediates such as $O_2.^-$ and $HO_2.$ are involved in the oxygen reduction process. The detailed mechanism for oxygen reduction remains unclear. In general, the electrochemical reduction of dioxygen shows a pronounced dependence on the electrode material and reaction medium [6,7]. Considering the fact that the oxygen–oxygen bond (O–O) in dioxygen molecule (O_2) requires higher bond dissociation energy than that in hydrogen peroxide (H_2O_2), it is difficult that oxygen reduction proceeds by direct four-electron pathway to give water. The electrode kinetics on carbon surfaces is much slower than those on active metals such as gold and platinum [8]. Xu et al. have investigated oxygen reduction on several different carbon surfaces, particularly polished and modified glassy carbon (GC) in alkaline solution [9]. They proposed the following mechanism

$$O_2 + e^- \rightarrow O_2^-{}_{\cdot(ads)} \quad (1)$$

$$O_2^-{}_{\cdot(ads)} + H_2O \rightarrow HO_2{}_{\cdot(ads)} + OH^- \quad (2)$$

$$HO_2. + O_2^-. \rightarrow HO_2^- + O_2 \quad (3)$$

or

$$HO_2{}_{\cdot(ads)} + e^- \rightarrow HO_2^-(aq) \quad (4)$$

They drew a conclusion that adsorption was critical to increasing the reduction rate by accelerating protonation of O_2^-. (Eq. (2)). Now, numerous studies focus on decreasing the overpotential of dioxygen reduction by chemically modified electrode. A variety of compounds have been used as electrocatalysts to modify the electrode surface, including some complexes of Cu^{2+} and Fe^{3+} [10,11], anthraquinone derivatives [12], Nafion-methylviologen [13] and some kinds of biomolecules such as cobalt porphyrins [14,15], catalase [16], vitamin B [17,18], cysteine [19] and

* Corresponding author. Department of Chemistry, Wuhan University, Wuhan 430072, PR China. Tel.: +86 27 8721 8904; fax: +86 27 6875 4067.
E-mail address: sshu@whu.edu.cn (S. Hu).

1567-5394/$ - see front matter © 2006 Elsevier B.V. All rights reserved.
doi:10.1016/j.bioelechem.2006.01.002

especially proteins [20,21], which show excellent electrocatalytic activity towards the electrochemical reduction of dioxygen. In our work, colloidal Au nanoparticles–deoxyribonucleic acid (Au_{nano}–DNA) composite film was used as electrode surface modification to improve the electrochemical responses of dissolved dioxygen. As far as Au nanoparticles are concerned, they play a key role in various applications such as biosensors and electrochemical sensors because of their unique electronic, optical, and catalytic properties [6,7,22–32]. Especially colloidal Au nanoparticles have been drawing attention from both theories and applications in modification of electrode surface. Many biomolecules mixed with colloidal Au nanoparticles can keep their biological activity well [33]. So Au nanoparticles have been successfully used to develop DNA and protein-sensing systems or other biosensors and electrochemistry sensors [22–26,34–36]. Yu et al. investigated that the presence of gold nanoparticles in the PE multilayers could significantly improve the electron-transfer characteristics of the films, which showed high electrocatalytic activity to the oxidation of nitric oxide (NO) [36]. In this paper, a Au_{nano}–DNA uniform film was fabricated on the glassy carbon electrode (GCE) surface. This Au_{nano}–DNA film electrode exhibited remarkable enhancement effects on the reduction of dioxygen in air-saturated 0.2 mol/L acetate buffer solution (pH = 5.2). A well-defined dioxygen reduction peak at about −0.24 V was observed and the overpotential decreased apparently compared with that at a bare GCE. This film was characterized by scanning electron microscopy (SEM) and transmission electron microscopy (TEM). Characteristic parameters and reaction mechanism for dioxygen reduction on the Au_{nano}–DNA film modified GCE were studied by rotating disk electrode voltammetry.

2. Experimental

2.1. Apparatus and reagents

All the electrochemical measurements were performed on a CHI 830 electrochemical analyzer (Shanghai Chenhua Co., China) in a three-electrode system. The working electrode was a Au_{nano}–DNA film coated GCE. A Pt wire and a saturated calomel electrode (SCE) were used as the counter and reference electrodes, respectively. The scanning electron microscopy (SEM) was performed with a Hitachi X-650 microscopy, and the transmission electron microscopy (TEM) images were obtained using a TEM-100 CXII (Japan) microscopy. For the nitrogen-saturated experiments, the electrolyte was bubbled with high-purity (99.999%) nitrogen for 6 min. Aurichloro-hydric acid ($HAuCl_4{\cdot}4\ H_2O$) was bought from Shanghai Chemical Reagents Co., Ltd. (China) and dissolved in doubly distilled water at a concentration of 10 mg/mL. The colloidal Au nanoparticles (Au_{nano}) were synthesized according to sodium citrate reduction method consulting corresponding reference [37]. 200 μL of 10 mg/mL $HAuCl_4{\cdot}4\ H_2O$ was mixed with 4.8 mL doubly distilled water, and then boiled in water bath with stirring successively. Finally 1.2 mL of 1% sodium citrate was dribbled into the boiling solution till the solution became red under the stirring condition, and then cooled in air. The synthesized Au_{nano} was blended with DNA stock solution according to the volume ratio of 2 : 1, and stored at 4 °C. Calf thymus DNA (CT DNA, gotten from Sigma, USA) was dissolved in water to form 0.8 mg/mL stock solution and stored at 4 °C. This solution of CT DNA gave a ratio of UV absorbance at 260 and 280 nm of 1.8–1.9 : 1, indicating that the DNA was sufficiently free of protein. The concentration of DNA solution, expressed in moles of base pair (BP, 2.558×10^{-3} mol/L), was determined by UV absorbance at 260 nm using the molar extinction coefficient (ε) of 13 200 $M^{-1}\ cm^{-1}$. Other chemicals used were analytical reagents. All the chemicals were used without further purification and all the solutions were prepared with doubly distilled water.

2.2. Preparation of the Au_{nano}–DNA film coated GCE

Prior to experiment, the GCE ($A = 0.071\ cm^2$) was mechanically polished with polishing microcloth containing 0.05 μm Al_2O_3 slurry to a mirror finish, and then carefully cleaned in 1 : 1 HNO_3–H_2O (v/v) and ethanol, water in turn via ultra-sonication each for 2 min. At last, 5 μL of the Au_{nano}–DNA solution was dropped on the GCE surface and air dried. Then a stable and uniform Au_{nano}–DNA film was formed. The modified electrode was dipped in doubly distilled water for several hours and air dried. In the same way, DNA film without Au_{nano} or Au_{nano} film without DNA coated GCE was obtained.

3. Results and discussion

3.1. SEM and TEM images of Au_{nano}

Fig. 1(a) and (b) shows the SEM images of Au_{nano} film and Au_{nano}–DNA film on the GCE surface. Apparently the Au_{nano} film without DNA is not uniform and the nanoparticles are easy to conglomerate (a). After the gold nanoparticles were mixed with DNA solution, the conglomeration effect was weakened markedly (b). The TEM images of Au_{nano} and Au_{nano}–DNA in solution support the above description as shown in Fig. 1(c) and (d). The globular morphology properties of Au_{nano} with average diameter of 15–20 nm are very clear and uniform (d) and conglomeration effect is serious (c). It is attributed to the fact that gold nanoparticles can adsorb on the long chains of DNA molecules. In other word, gold nanoparticles were dispersed perfectly by the DNA molecules avoiding the process of conglomerating.

3.2. Cyclic voltammetry

The cyclic voltammograms of dioxygen in 0.2 mol/L air-saturated acetate buffer solution (pH = 5.2) at different electrodes are shown in Fig. 2 when the potential initially sweeps from 1.30 to −0.80 V. Curves a and b show the electrochemical behaviors of dioxygen at Au_{nano}–DNA film modified GCE in the air-saturated solution and nitrogen-bubbled solution, respectively. Apparently, a pair of redox peaks can be observed at about 1.15 and 0.54 V, which are attributed to the oxidation–reduction of the Au_{nano}, and a well-defined dioxygen reduction

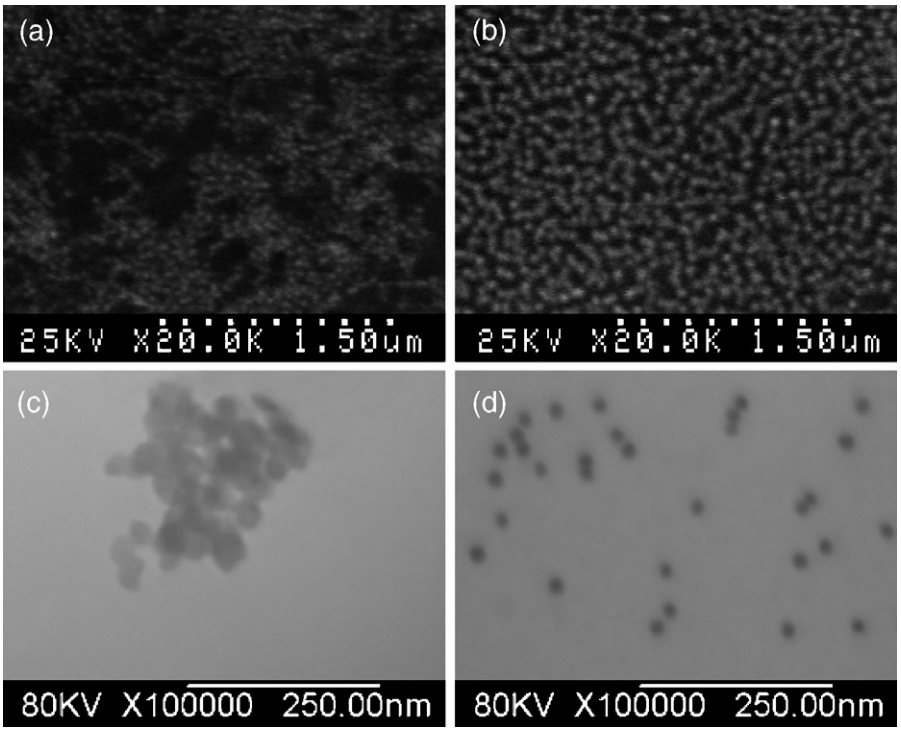

Fig. 1. SEM images of Au_{nano} film (a) and Au_{nano}–DNA film (b) on the GCE surface, and the TEM images of Au_{nano} (c) and Au_{nano}–DNA (d) in solutions.

peak appears at about −0.24 V (curve a) at this modified GCE. It is clear that the dioxygen reduction is irreversible. Compared with the reduction peak current in curve a, the smart decrease but not disappearance of that in curve b at about −0.24 V indicates that the dioxygen elimination via nitrogen bubbling for 6 min is effective but not satisfying, and confirms that the reduction peak is due to dioxygen. However, the redox peak potentials of Au_{nano} shift a little positively in air-saturated solution (curve a) compared with those in nitrogen-bubbled solution (curve b). Based on this fact, it is concluded that the presence of dioxygen has a slight effect on the redox of Au_{nano} and some interaction may be present between Au_{nano} and dioxygen. At DNA film modified electrode (curve d), there is not any peak in the range of potential from 1.40 to −0.80 V indicating that DNA can block the electron transfer between oxygen molecules and the electrode surface. Nevertheless, only one reduction peak appears at about −0.68 V at bare GCE (curve c). It can be seen that the modified electrode shows excellent enhancement effect on the reduction of dioxygen with lower overpotential than that at bare GCE. The structure of gold nanoparticles dispersed in Au_{nano}–DNA film can provide more active sites and contact more dioxygen molecules to increase the peak current of dioxygen reduction.

3.3. The volume ratio of DNA vs. Au_{nano}

The influences of volume ratio of DNA vs. Au_{nano} on the reduction peak currents and peak potentials are evaluated by using linear sweep voltammetry (LSV). The data are depicted in Fig. 3a and b, respectively. When the ratio is 1:2, the reduction peak current of dioxygen comes to a head and the peak potential is the most positive. However those of Au_{nano} do not obey a specific rule. Generally with the decrease of the ratio the current increases slowly. This experiment phenomenon may be attributed to the saturated adsorption of Au_{nano} on the DNA molecules at the values of 1:2, and then further adsorption of Au_{nano} produces negative effects on the reduction of dioxygen even though the amount of Au_{nano} increases, whereas the state of being conglomerated increases subsequently. Accordingly, the interaction manner between the gold nanoparticles and dioxygen molecules changes and effective active sites reduce.

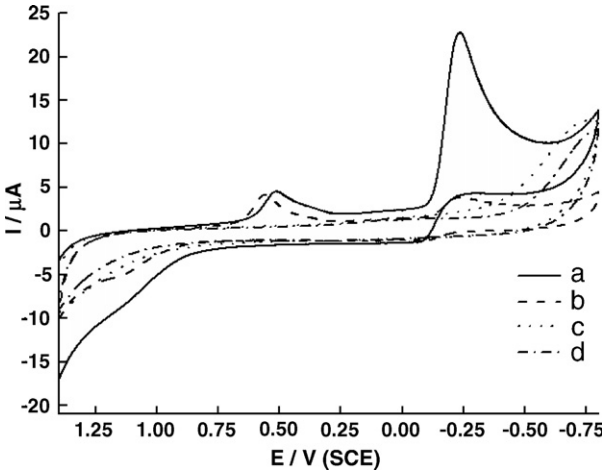

Fig. 2. Cyclic voltammograms of dioxygen in 0.2 mol/L air-saturated acetate buffer solution (pH=5.2) at Au_{nano}–DNA film modified GCE in the air-saturated solution (a) and in nitrogen-bubbled solution (b), bare GCE (curve c) and DNA film modified GCE (curve d). Scan rate, 100 mV/s.

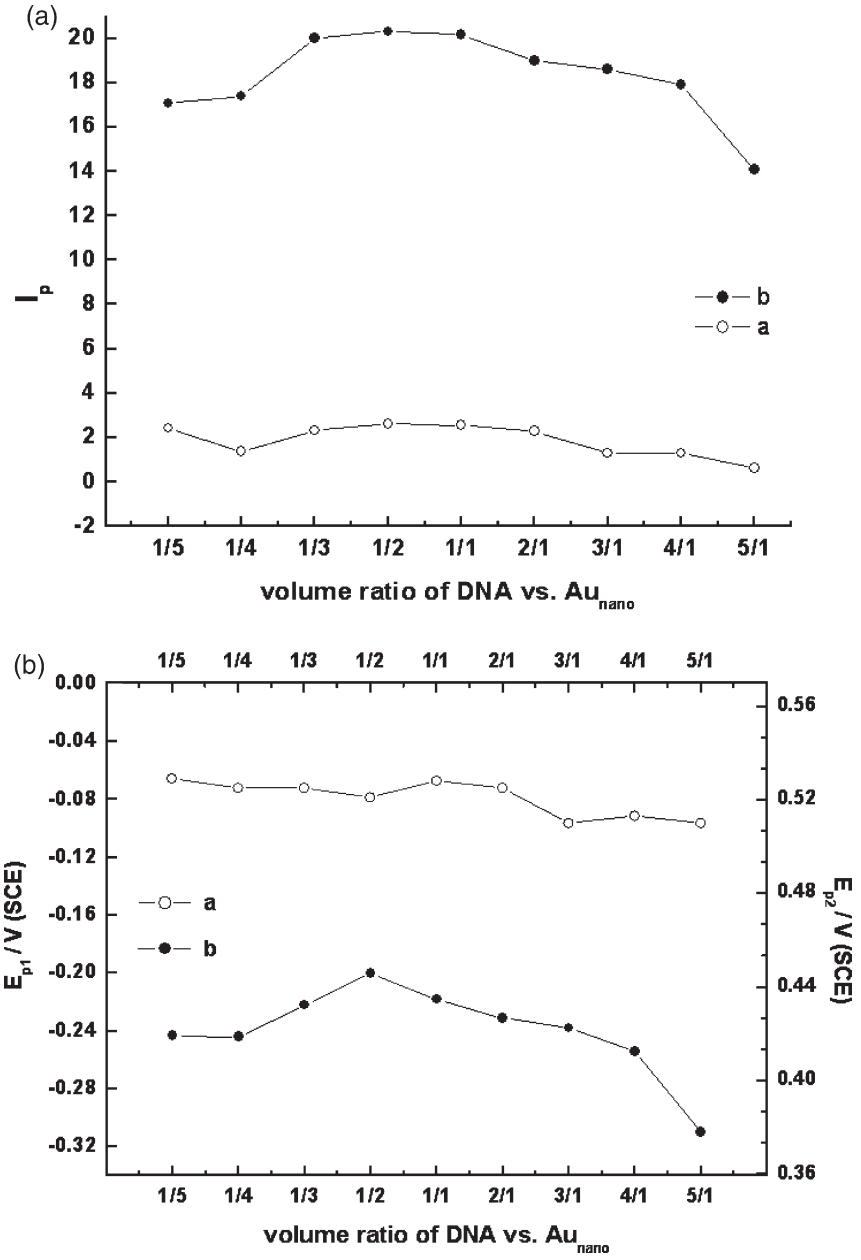

Fig. 3. The influences of volume ratio of DNA vs. Au_{nano} on the reduction peak currents (a) and peak potentials (b) by using linear sweep voltammetry. Scan rate, 100 mV/s.

3.4. The effects of scan rate

The linear sweep voltammetric responses of dioxygen at Au_{nano}–DNA film coated GCE at various scan rates were investigated in 0.2 mol/L acetate buffer solution (pH=5.2) saturated with air. The experiment data are exhibited in the Fig. 4. Fig. 4a describes the relationship between the reduction peak currents (I_p) and the scan rate (v) ranging between 0.05 and 0.50 V/s. It is clear that the current of dioxygen reduction (R1) is proportional to the square root of scan rate (b in Fig. 4a), which is described by the following equation:

$$I_p(\mu A) = 53.066v^{1/2} + 5.724 (R = 0.9988) \quad (5)$$

denoting diffusion-controlled processes for the reduction of dioxygen at Au_{nano}–DNA film coated GCE.

Thus, the peak current of gold nanoparticles reduction linearly increased with the increase of scan rate that ranged from 0.05 to 0.50 V/s obeying the equation as follows (a in Fig. 4a):

$$I_p(\mu A) = 8.945v + 0.200 (R = 0.9946) \quad (6)$$

indicating that the gold nanoparticles reduction is a surface electrochemical reaction.

Fig. 4b explains the effects of scan rate on the peak potentials (E_p, V) (curve a for Au_{nano}, curve b for O_2). As an irreversible reaction, the peak potentials shift negatively with the increase of

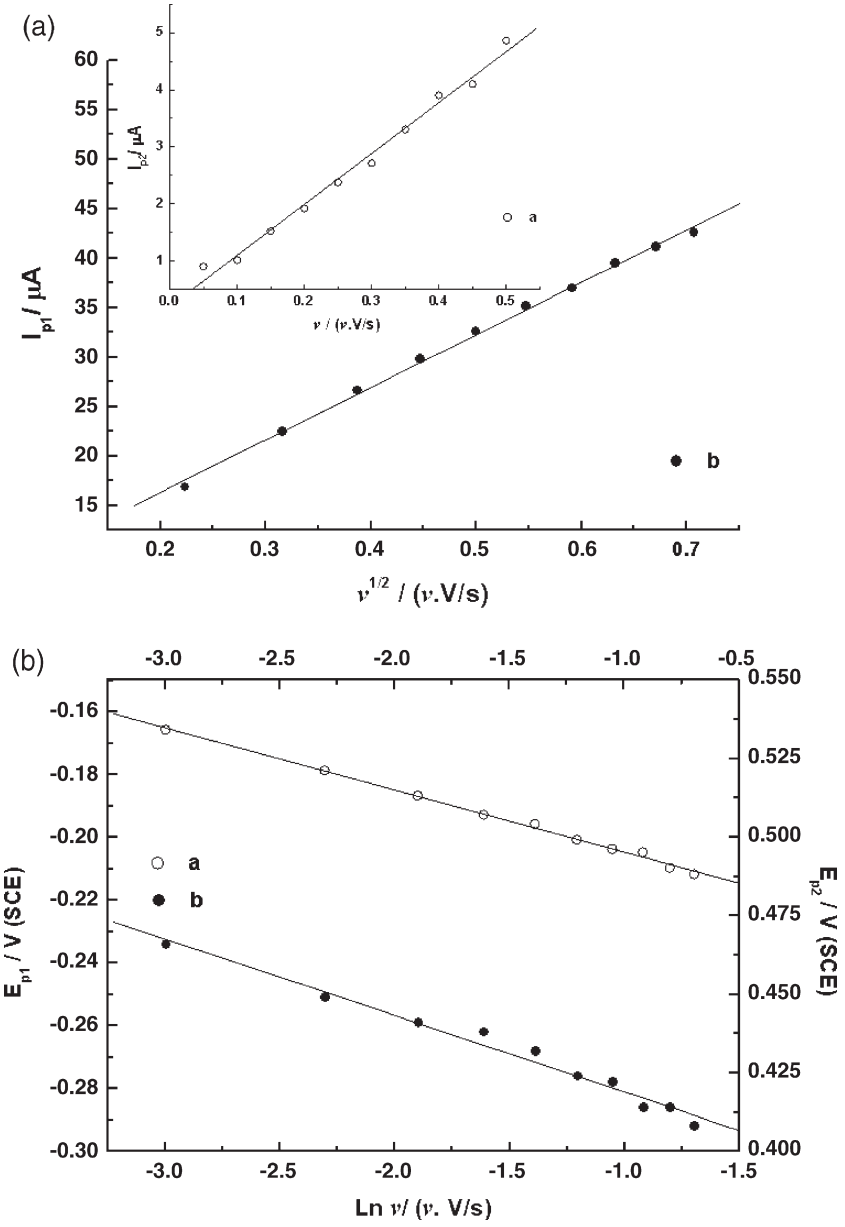

Fig. 4. The effects of scan rates using linear sweep voltammetry on peak currents (a) and peak potentials (b).

scan rate and have linear relationships with the natural logarithm of scan rate (V/s). The peak potential of dioxygen reduction changes according to the following equation:

$$E_p(\mathrm{V}) = -0.025\ln v - 0.305 (R = 0.9897) \quad (7)$$

Because the dioxygen reduction process is controlled by the diffusion of dioxygen, based on the traditional theory [38] the value of αn_a can be calculated from the slope of above equation. Where α is the transfer coefficient and n_a is the number of electron transferred in the rate-limiting step. According to the experiment results, the value of αn_a is calculated as 0.48. Considering the reasonable value range of α_1 from 0.2 to 0.7, the acceptable number of electron involved in the reduction of dioxygen at Au_{nano}–DNA film electrode is one. That is to say, one electron is involved in the rate-limiting step of reduction reaction of dioxygen, the value of α_1 is 0.48 correspondingly.

However, as to the irreversible surface electrochemical reaction, the relationship between the scan rate v (V/s) and the peak potential E_p (V) can be expressed by the following equation [39]:

$$E_p(\mathrm{V}) = E^{0'} + (RT/\alpha n_a F)\ln(RTk_s/\alpha n_a F) + (RT/\alpha n_a F)\ln v \quad (8)$$

where k_s is the rate coefficient of the surface reaction, and $E^{0'}$ (V) is the formal potential which can be obtained from the intercept of the E_p (V) vs. v (V/s) curve by extrapolation to the vertical axis at v=0.0 V/s. Other symbols have their usual significance.

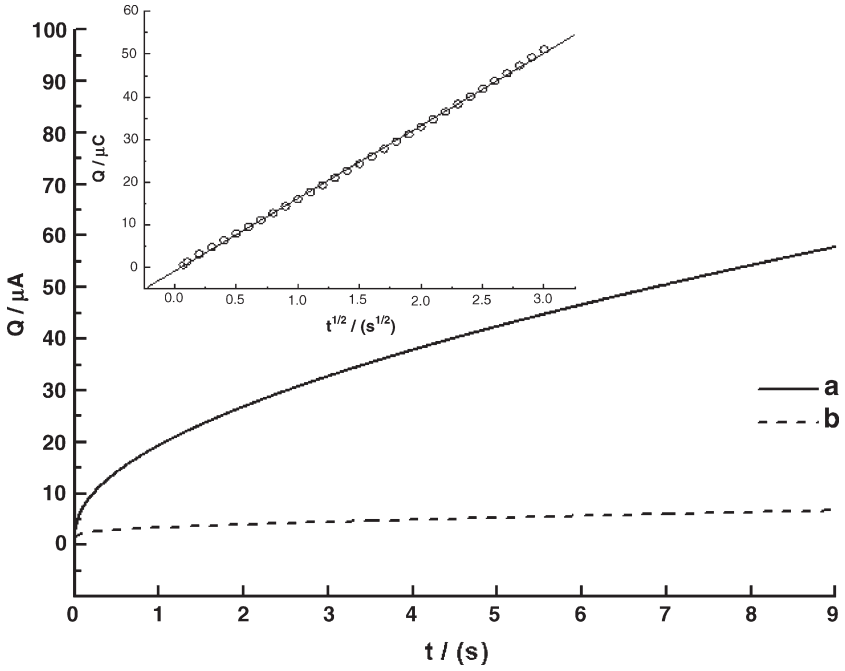

Fig. 5. Chronocoulometric responses of dioxygen at Au_{nano}–DNA film modified GCE in 0.2 mol/L air-saturated acetate buffer solution (pH=5.2) (curve a). Curve b stands for that in nitrogen-saturated solution. The inset shows the linear relationship between the charges (Q) and the square roots of times ($t^{1/2}$) for the reduction reaction of dioxygen (background subtracted). Pulse width 9 s.

Similarly, the relationship between the peak potential of Au_{nano} (E_p (V)) and scan rate (v (V/s)) can be expressed by following formula:

$$E_p(V) = -0.0198 \ln v + 0.475 (R = 0.9982) \quad (9)$$

Thus from the slope and intercept of the E_p (V) vs. ln v (V/s) plot the values of αn_a can be calculated as 1.29. The acceptable number of electron involved in rate-limiting step in Au_{nano} reduction is 2.6 if the value of α is 0.5.

3.5. Chronocoulometry

The method of chronocoulometry was applied to characterize the electrochemical reduction of dioxygen at Au_{nano}–DNA

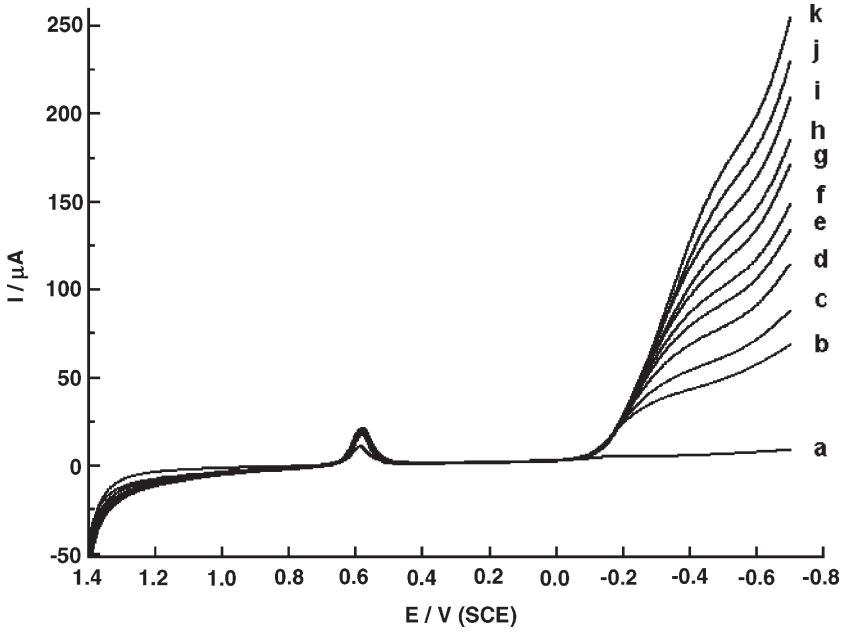

Fig. 6. Current–potential curves at a rotating modified GCE in 0.2 mol/L acetate buffer solution (pH=5.2) in the absence of dioxygen at rotating rate 200 rpm (a) and at different rotating rates in air-saturated solution (b–k): (b) 100; (c) 200; (d) 400; (e) 600; (f) 800; (g) 1100; (h) 1400; (i) 1800; (j) 2300; (k) 2800 rpm, for each voltammogram potential scan rate 10 mV/s.

film modified electrode in 0.2 mol/L air-saturated acetate buffer solution (pH=5.2). The results are displayed in Fig. 5. After the subtraction of the background charge, which can eliminate the effect of double-layer charge in our experiment, the plots of Q (μC) against t (s) in Fig. 5 are converted into the plots of Q against $t^{1/2}$. It is obvious that the charges (Q) have linear relationships with the square roots of time ($t^{1/2}$) for the first reaction of dioxygen reduction (inset in Fig. 5). According to the integrated Cottrell equation, the number of electron involved in the reduction of dioxygen can be estimated from the slope of the plot of Q vs. $t^{1/2}$.

$$Q = 2nFAcD^{1/2}\pi^{-1/2}t^{1/2} \tag{10}$$

where n is the number of electron involved in reduction of dioxygen, F is Faraday constant, A is the electrode area, c is the concentration of dioxygen in air-saturated solution [40], D is the diffusion coefficient of dioxygen in aqueous solution. Other symbols have their usual significance. In this work, $A=0.071$ cm^2, $c=0.25\times10^{-3}$ mol/L, and slope is 16.49 μC s$^{-1/2}$. On the assumption that the value of D is 1.51×10^{-5} cm^2 s^{-1} [41], it is calculated that the number of electron involved in the electrochemical reduction dioxygen is 2. It is estimated that the reduction product of dioxygen is H_2O_2.

3.6. Rotating disk electrode and rotating ring-disk electrode measurements

Dioxygen reduction is a complex reaction that involved many reaction intermediates. So rotating disk electrode (RDE) and rotating ring-disk electrode (RRDE) voltammetry have been used for the further research on the mechanism of the electrochemical reduction of dioxygen.

Fig. 6 illuminates RDE results for the Au_{nano}–DNA film modified glassy carbon rotating disk electrode in 0.2 mol/L air-saturated acetate buffer solution (pH=5.2) at different rotation rates. From the disk currents–disk potential curves recorded by linear scan from 1.40 to −0.70 V, it can be seen that the limiting current I_L (μA) of dioxygen, which is defined as the difference between the currents on the modified electrode in deaerated and those in air-saturated solutions, increases with the increase of rotation rate as a diffusion-controlled electrode process. The reduction peak at about 0.57 V is due to the reduction of gold nanoparticles, which is a surface electrochemical reaction, and its currents do not change with the changes of rotation rate. However, the current reduces apparently and the potential shifts positively slightly in deaerated solutions compared to those in air-saturated solution. These results are consistent with that obtained from the above discussion in Section 3.1.

Based on the RDE data obtained in the present study, the Koutecky–Levich plots for reduction of dioxygen at the Au_{nano}–DNA film modified electrode are drawn in Fig. 7 offering more kinetics information. Under the conditions of high rotation rates, the slopes of the plots at different disk potentials are almost the same. The diffusion limiting current I_D (μA) can be determined according to the Koutecky–Levich equation formulated as follows:

$$\frac{1}{I_L} = \frac{1}{I_K} + \frac{1}{I_D} \tag{11}$$

where I_K (μA) is kinetics current, namely current controlled by the surface electrochemical reaction process, and I_D (μA) is the corresponding diffusion limiting current obtained on the basis of the Levich equation described as follows:

$$I_D(\mu A) = 0.62nFAD^{2/3}\upsilon^{-1/6}c_{O_2}\omega^{1/2} \tag{12}$$

here υ is the kinematic viscosity, ω is the angular frequency of rotation (rpm), A is the disk electrode area. Other symbols have

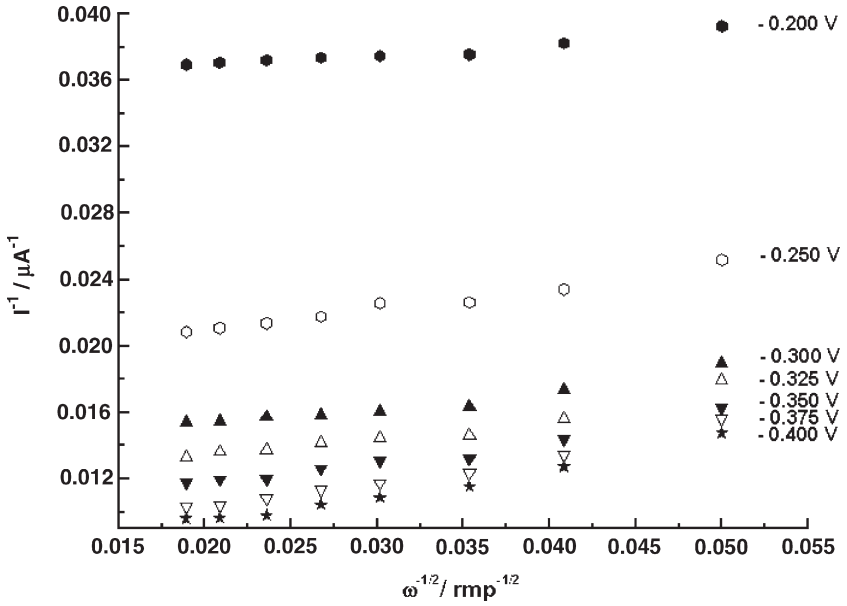

Fig. 7. Koutecky–Levich plots for the electrochemical reduction of dioxygen at the Au_{nano}–DNA film modified electrode in 0.2 mol/L air-saturated acetate buffer solution (pH=5.2). Scan rate 10 mV/s.

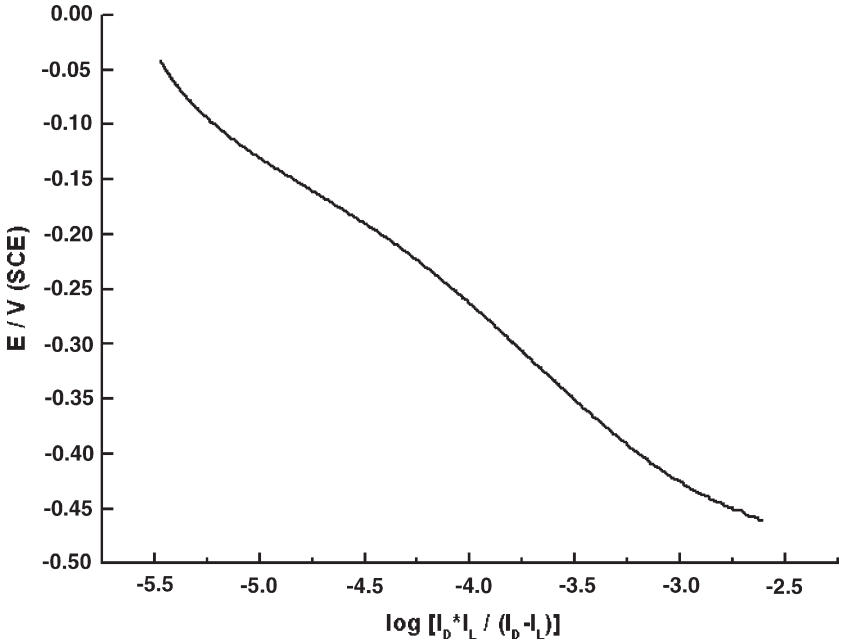

Fig. 8. Tafel plot constructed from corrected disk currents for the reduction reaction in 0.2 mol/L air-saturated acetate buffer solution (pH=5.2). Scan rate 10 mV/s, rotation rate 800 rpm.

their conventional meanings. The value of kinematic viscosity of water and the concentration of O_2 in solution are 0.01 cm^2/s and 0.25×10^{-3} mol/L, respectively. $A=0.273$ cm^2. Based on the slopes of the Koutecky–Levich plots, the number of electrons transferred in reduction processes of dioxygen at Au_{nano}–DNA film modified electrode is close to the theoretical values of 2 according to the Levich equation. This result is consistent with that calculated from chronocoulometry data. Moreover, based on the following equation deduced from the Koutecky–Levich equation,

$$I_K = \frac{I_D \cdot I_L}{I_D - I_L} \tag{13}$$

Tafel plot is obtained from the corrected disk current at rotation rate of 800 rpm (Fig. 8). In another way, I_K at different disk potentials can be calculated directly from the intercepts of

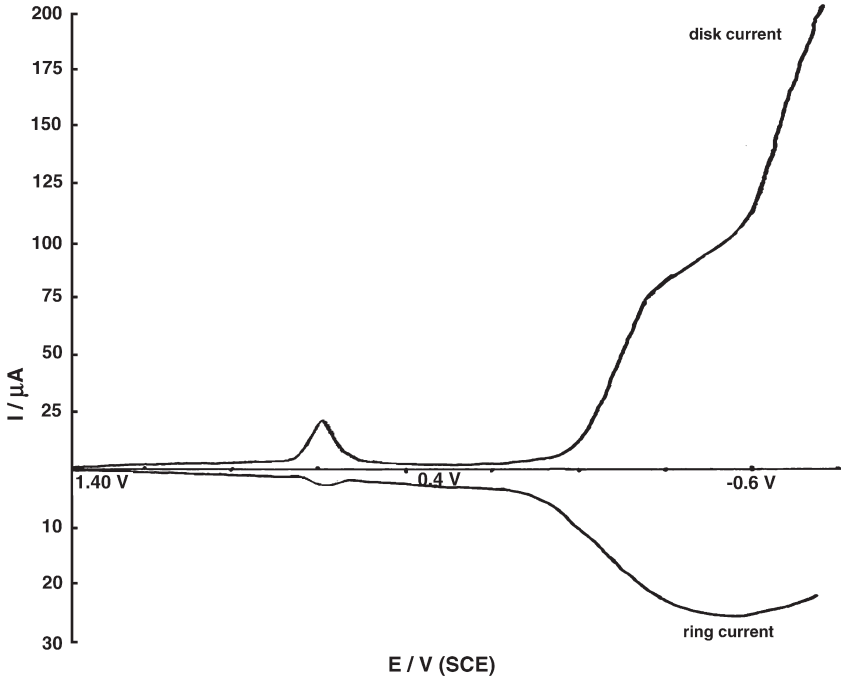

Fig. 9. The comparison of currents at the Au_{nano}–DNA film modified electrode at a rotating rate of 800 rpm in 0.2 mol/L air-saturated acetate buffer solution (pH=5.2). The oxidation potential used to detect peroxide was set at 1.0 V. For disk current voltammogram potential scan rate 10 mV/s. Collection efficiency N is 0.11.

Koutecky–Levich plots, and then the plot of disk potential vs. logarithm of I_K is drawn and its slope is traditional Tafel slope. From the data in Fig. 8, the number transferred in rate-limiting step of the electrochemical reduction of dioxygen is obtained. Based on the Tafel equation, the value of αn_a can be calculated as 0.41. Here, n_a is 1 then the α is 0.41. This outcome supports the finding obtained by scan rate analysis using LSV.

Otherwise, the RRDE was employed to determine the product of dioxygen reduction at a rotation rate of 800 rpm in 0.2 mol/L air-saturated acetate buffer solution (pH = 5.2). The disk and ring currents as a function of the disk potential for dioxygen reduction are recorded in Fig. 9. The operating potential of the ring is 1.0 V. With emergence of the diffusion limiting current plateau of disk current, the ring current comes to a head then drops, suggesting that the electrochemical reduction of dioxygen at this modified electrode gives hydrogen peroxide (H_2O_2) via accepting two electrons, which is swept away from the rotating disk electrode and then reduced at the ring electrode. At high enough disk potential, H_2O_2 may be further reduced to water or decompose to form water and dioxygen subsequently, which results in the increase of disk current and the decrease of ring current correspondingly. As for the ill-defined peak at about 0.60 V in the ring current curve, it is attributed to the redox of Au colloid immobilized on the electrode surface.

3.7. Reaction mechanism

The electrochemical reduction process of dioxygen at Au_{nano}–DNA film coated GCE in 0.2 mol/L acetate buffer solution (pH 5.2) saturated with air has been studied and the number of electron transferred in the reaction has been calculated. The experimental data show that only one electron is involved in the rate-limiting step for the reduction reaction of dioxygen. Thus the possible mechanism for the electrochemical reduction of dioxygen can be described as follows:

$$O_2 + e^- \rightarrow O_2^-(\text{rate} - \text{limiting step}) \quad (14)$$

$$O_2^- + H_2O + e^- \rightarrow O_2H^- + OH^-. \quad (15)$$

4. Conclusion

A Au_{nano}–DNA film modified GC electrode was developed to study the electrochemical reduction of dioxygen. The reaction mechanisms of the dioxygen reduction were explained by using electrochemical technique. All experiment results demonstrate that two electrons are involved in whole reduction process, but it is not a direct pathway. It proceeds through two steps. One is the step of one-electron reduction to superoxide ion and the other is the further reduction of superoxide ion to hydrogen peroxide involving one electron transfer as rate-limiting step. The present conclusion is confirmed by RDE and RRDE research. Moreover, the transfer coefficient for the rate-limiting step of dioxygen reduction is determined.

Acknowledgments

This research is supported by the National Natural Science Foundation of China (No. 30370397 and 60571042).

References

[1] E. Yeager, Recent advances in the science of electrocatalysis, J. Electrochem. Soc. 128 (1981) 160C–171C.
[2] N.M. Markovic, H.A. Gasteiger, P.N. Ross, Kinetics of oxygen reduction on Pt (hkl) electrodes: implications for the crystallite size effect with supported Pt electrocatalysts, J. Electrochem. Soc. 144 (1997) 1591–1597.
[3] O. Solorza-Feria, S. Citalan-Cigarroa, R. Rivera-Noriego, S.M. Fernandez-Valverde, Oxygen reduction in acid media at the amorphous Mo–Os–Se carbonyl cluster coated glassy carbon electrodes, Electrochem. Commun. 1 (1999) 585–589.
[4] J.C. Huang, R.K. Sen, E. Yeager, Oxygen reduction on platinum in 85% orthophosphoric acid, J. Electrochem. Soc. 126 (1979) 786–792.
[5] C.C. Wang, K.S. Goto, S.A. Akbar, Demixing of (Ni, Co)O under an oxygen potential gradient using a YSZ-based galvanic cell, J. Electrochem. Soc. 138 (1991) 3673–3677.
[6] J. Prakash, H. Joachin, Electrocatalytic activity of ruthenium for oxygen reduction in alkaline solution, Electrochim. Acta., 45 (2000) 2289. Pages 2289–2296.
[7] T.J. Schmidt, V. Stamenković, M. Arenz, N.M. Marković, P.N. Ross Jr., Oxygen electrocatalysis in alkaline electrolyte: Pt (hkl), Au (hkl) and the effect of Pd-modification, Electrochim. Acta 47 (2002) 3765–3776.
[8] H.H. Yang, R.L. McCreery, Elucidation of the mechanism of dioxygen reduction on metal-free carbon electrodes, J. Electrochem. Soc. 147 (2000) 3420–3428.
[9] J. Xu, W.H. Huang, R.L. McCreery, Isotope and surface preparation effects on alkaline dioxygen reduction at carbon electrodes, J. Electroanal. Chem. 410 (1996) 235–242.
[10] J. Zhang, F.C. Anson, Electrochemistry of the Cu (II) complex of 4, 7-diphenyl-1, 10-phenanthrolinedisulfonate adsorbed on graphite electrodes and its behavior as an electrocatalyst for the reduction of O_2 and H_2O_2, J. Electroanal. Chem. 341 (1992) 323–341.
[11] J. Zhang, F.C. Anson, Complexes of Cu (II) with electroactive chelating ligands adsorbed on graphite electrodes: surface coordination chemistry and electrocatalysis, J. Electroanal. Chem. 348 (1993) 81–97.
[12] S.M. Golabi, J.B. Baoof, Catalysis of dioxygen reduction to hydrogen peroxide at the surface of carbon paste electrodes modified by 1, 4-naphthoquinone and some of its derivatives, J. Electroanal. Chem. 416 (1996) 75–82.
[13] S.S. Hu, Electrocatalytic reduction of molecular oxygen on a sodium montmorillonite-methyl viologen carbon paste chemically modified electrode, J. Electroanal. Chem. 463 (1999) 253–257.
[14] C. Shi, B. Steiger, M. Yuasa, F.C. Anson, Electroreduction of O_2 to H_2O at unusually positive potentials catalyzed by the simplest of the cobalt porphyrins, Inorg. Chem. 36 (1997) 4294–4295.
[15] C. Shi, F.C. Anson, (5, 10, 15, 20-Tetramethylporphyrinato)cobalt(II): a remarkably active catalyst for the electroreduction of O_2 to H_2O, Inorg. Chem. 37 (1998) 1037–1043.
[16] M.E. Lai, A. Bergel, Eletrochemical reduction of oxygen on glassy carbon: catalysis by catalase, J. Electroanal. Chem. 494 (2000) 30–40.
[17] J. Zhang, F.C. Anson, Coordination of Fe^{3+} by "alizarin complexone" adsorbed on graphite electrodes to produce electrocatalysts for the reduction of O_2 and H_2O_2, J. Electroanal. Chem. 353 (1993) 265–280.
[18] J.H. Zagal, M.J. Auirre, M.A. Paez, O_2 reduction kinetics on a graphite electrode modified with adsorbed vitamin B_{12}, J. Electroanal. Chem. 437 (1997) 45–52.
[19] M.S. El-Deab, T. Ohsaka, Quasi-reversible two-electron reduction of oxygen at gold electrodes modified with a self-assembled submonolayer of cysteine, Electrochem. Commun. 5 (2003) 214–219.

[20] Q. Wang, G. Lu, B. Yang, Myoglobin/sol–gel film modified electrode: direct electrochemistry and electrochemical catalysis, Langmuir 20 (2004) 1342–1347.
[21] A.S. Haas, D.L. Pilloud, K.S. Reddy, G.T. Babcock, C.C. Moser, J.K. Blasie, P.L. Dutton, Cytochrome *c* and cytochrome *c* oxidase: monolayer assemblies and catalysis, J. Phys. Chem., B 105 (2001) 11351–11362.
[22] J. Wang, R. Polsky, D. Xu, Silver-enhanced colloidal gold electrochemical stripping detection of DNA hybridization, Langmuir 17 (2001) 5739–5741.
[23] M. Ozsoz, A. Erdem, K. Kerman, D. Ozkan, B. Tugrul, N. Topcuoglu, H. Ekren, M. Taylan, Electrochemical genosensor based on colloidal gold nanoparticles for the detection of factor V leiden mutation using disposable pencil graphite electrodes, Anal. Chem. 75 (2003) 2181–2187.
[24] J. Wang, D. Xu, R. Polsky, Magnetically-induced solid-state electrochemical detection of DNA hybridization, J. Am. Chem. Soc. 124 (2002) 4208–4209.
[25] S.J. Park, T.A. Taton, C.A. Mirkin, Array-based electrical detection of DNA with nanoparticle probes, Science 295 (2002) 1503–1506.
[26] O. Lioubashevski, V.I. Chegel, F. Patolsky, E. Katz, I. Willner, Enzyme-catalyzed bio-pumping of electrons into Au-nanoparticles: a surface plasmon resonance and electrochemical study, J. Am. Chem. Soc. 126 (2004) 7133–7143.
[27] H. Ye, R.M. Crooks, Electrocatalytic O_2 reduction at glassy carbon electrodes modified with dendrimer-encapsulated Pt nanoparticles, J. Am. Chem. Soc. 127 (2005) 4930–4934.
[28] C.M. Niemeyer, Nanoparticles, proteins, and nucleic acids: biotechnology meets materials science, Angew. Chem., Int. Ed. Engl. 40 (2001) 4128–4158.
[29] A.N. Shipway, E. Katz, I. Willner, Nanoparticle arrays on surfaces for electronic, optical, and sensor applications, Chem. Phys. Chem. 1 (2000) 18–52.
[30] P.V. Kamat, Photophysical, photochemical and photocatalytic aspects of metal nanoparticles, J. Phys. Chem., B 106 (2002) 7729–7744.
[31] W. Shenton, S.A. Davis, S. Mann, Directed self-assembly of nanoparticles into macroscopic materials using antibody–antigen recognition, Adv. Mater. 11 (1999) 449–452.
[32] H. Cai, C. Xu, P.G. He, Y.Z. Fang, Colloid Au-enhanced DNA immobilization for the electrochemical detection of sequence-specific DNA, J. Electroanal. Chem. 510 (2001) 78–85.
[33] D. Hernández-Santos, M.B. González-Garćýa, A. Costa-Garćýa, Metal-nanoparticles based electroanalysis, Electroanalysis 14 (2002) 1225–1235.
[34] P.C. Biswas, Y. Nodasaka, M. Haruta, Electro-oxidation of CO and methanol on graphite-based platinum electrodes combined with oxide-supported ultrafine gold particles, J. Electroanal. Chem. 381 (1995) 167–177.
[35] M. Valden, X. Lai, D.W. Goodman, Onset of catalytic activity of gold clusters on titania with the appearance of nonmetallic properties, Science 281 (1998) 1647–1650.
[36] A.M. Yu, Z.J. Liang, J.H. Cho, F. Caruso, Nanostructured electrochemical sensor based on dense gold nanoparticle films, Nano Lett. 3 (2003) 1203–1207.
[37] Y.H. Wu, S.S. Hu, The fabrication of a colloidal gold-carbon nanotubes composite film on a gold electrode and its application for the determination of cytochrome *c*, Colloids Surf., B Biointerfaces 41 (2005) 299–304.
[38] E. Laviron, General expression of the linear potential sweep voltammogram in the case of diffusionless electrochemical systems, J. Electroanal. Chem. 101 (1979) 19–28.
[39] F.C. Anson, Application of potentiostatic current integration to the study of the adsorption of cobalt (III)-ethylenedinitrilo(tetraacetate) on mercury electrodes, Anal. Chem. 36 (1964) 932–934.
[40] A.J. Bard, L.R. Faulkner, Electrochemical Methods: Fundamentals and Application, 2nd ed., John Wiley & Sons, Inc., New York, 2001, p. 304.
[41] D.H. Evans, J.J. Lingane, The chronopotentiometric reduction of oxygen at gold electrodes, J. Electroanal. Chem. 6 (1963) 283–299.